Filtered POD based low dimensional modeling of the 3D turbulent flow behind a circular cylinder

Article *in* International Journal for Numerical Methods in Fluids · May 2011

DOI: 10.1002/fld.2238

5 authors, including:

Stefan Siegel
Atargis Energy Corporation
108 PUBLICATIONS **869** CITATIONS
SEE PROFILE

Kelly Cohen
University of Cincinnati
214 PUBLICATIONS **1,035** CITATIONS
SEE PROFILE

INTERNATIONAL JOURNAL FOR NUMERICAL METHODS IN FLUIDS
Int. J. Numer. Meth. Fluids (2010)
Published online in Wiley InterScience (www.interscience.wiley.com). DOI: 10.1002/fld.2238

Filtered POD-based low-dimensional modeling of the 3D turbulent flow behind a circular cylinder

Selin Aradag[1,*,†,‡], Stefan Siegel[2,§], Jürgen Seidel[2,§], Kelly Cohen[3,¶] and Thomas McLaughlin[4,‖]

[1]*TOBB University of Economics and Technology, Ankara 06560, Turkey*
[2]*Department of Aeronautics, US Air Force Academy, CO 80840, U.S.A.*
[3]*Department of Aerospace Engineering, University of Cincinnati, Cincinnati, OH 45221-0070, U.S.A.*
[4]*Aeronautics Research Center, Department of Aeronautics, US Air Force Academy, CO 80840, U.S.A.*

SUMMARY

Low-dimensional models have proven essential for feedback control and estimation of flow fields. While feedback control based on global flow estimation can be very efficient, it is often difficult to estimate the flow state if structures of very different length scales are present in the flow. The conventional snapshot-based proper orthogonal decomposition (POD), a popular method for low-order modeling, does not separate the structures according to size, since it optimizes modes based on energy. Two methods are developed in this study to separate the structures in the flow based on size. One of them is Hybrid Filtered POD method and the second one is 3D FFT-based Filtered POD approach performed using a fast Fourier transform (FFT)-based spatial filtering. In both the methods, a spatial low-pass filter is employed to precondition snapshot sets before deriving POD modes. Three-dimensional flow data from the simulation of turbulent flow over a circular cylinder wake at $Re = 20000$ is used to evaluate the performance of the two methods. Results show that both the FFT-based 3D Filtered POD and Hybrid Filtered POD are able to capture the large-scale features of the flow, such as the von Karman vortex street, while not being contaminated by small-scale turbulent structures present in the flow. Copyright © 2010 John Wiley & Sons, Ltd.

Received 10 March 2009; Revised 28 September 2009; Accepted 1 October 2009

KEY WORDS: von Karman vortex street; vortex shedding; low-dimensional modeling; proper orthogonal decomposition; cylinder wake; filtered POD; hybrid POD

1. INTRODUCTION

The phenomenon of vortex shedding behind bluff bodies has been a subject of extensive research. Many flows of engineering interest produce this phenomenon and the associated periodic lift and drag response. Applications include aircraft and missile aerodynamics, marine structures, underwater acoustics, civil and wind engineering [1]. The control of the wake behind bluff bodies has been crucial in several engineering applications during the past few decades. Especially, active

*Correspondence to: Selin Aradag, TOBB University of Economics and Technology, Ankara 06560, Turkey.
†E-mail: selinaradag@gmail.com
‡Assistant Professor.
§Visiting Researcher.
¶Associate Professor.
‖Director.

Contract/grant sponsor: Air Force Office of Scientific Research; contract/grant number: FA-955005C0048

feedback control to reduce the drag on vehicles has been a very important area of research since drag reduction is directly related to energy saving.

Feedback of flow fields using low-dimensional models has been shown to be much more effective than *ad hoc* approaches [2–8]. Its feasibility depends to a large degree on the ability to estimate the state-of-the-flow field in real time. In comparison to earlier attempts that used 'black box' controllers [8], which do not include any flow field model at all, a low-dimensional model-based controller employs a mathematical representation of the flow both for controller development and real-time flow state estimation.

For controllers to be able to target individual structures in the flow, the model needs to have the inherent ability to identify them. While the conventional snapshot-based proper orthogonal decomposition (POD) successfully accomplishes this for two-dimensional laminar flows, where the energy drop-off for higher order modes is rather steep, turbulent three-dimensional flows pose additional problems [9]. In these flows, the flow energy is transferred rather quickly towards smaller scales, which are energetic and random. As a result, the energy drop-off for turbulent flows is a lot less steep, and each of the resulting POD modes contains structures of different sizes. This necessitates that many more modes have to be retained in the truncated model in order to cover a given portion of the energy of the flow. Furthermore, the resulting modes do not distinguish between flow structures of different length scales. The resulting POD modes are therefore not easily usable as controller input, since typically controller parameters depend on frequency and hence structure size.

A circular cylinder is a well-studied and documented benchmark for a bluff body wake problem. The near wake for the flow past a circular cylinder determines the dominant instability in the flow, which leads to the vortex street formation [10]. It is also responsible for the secondary instability and the subsequent bifurcations that lead to a turbulent state, as found both computationally [11] and experimentally [12]. A technique was pioneered by Ma and Karniadakis [9] for the circular cylinder wake to overcome the difficulties related to low-dimensional modeling of the circular cylinder wake. They demonstrate that a combination of 2D and 3D modes obtained from the flows at different Reynolds numbers (hybrid modes) lead to a better numerical model of the cylinder wake.

2. RESEARCH OBJECTIVES

For controllers to be able to target individual structures in the flow, the structures that will be controlled first need to be identified. The main aim of the current study is to develop and evaluate methods that are able to identify the large-scale two-dimensional structures that constitute the von Karman vortex street for a turbulent three-dimensional cylinder wake by separating these structures from the rest of the flow, which includes streamwise vortices and small-scale turbulent fluctuations. There are two methods developed and used in this study for this purpose. One of them is a Hybrid Filtered POD procedure inspired by the hybrid POD approach of Ma and Karniadakis [12] and the second one is a 3D FFT-based Filtered POD approach performed using a fast Fourier transform (FFT)-based spatial filtering.

The investigation uses data from three-dimensional turbulent simulations of a circular cylinder wake at a Reynolds number of 20 000. This flow field has a number of features that make it very suitable for this type of investigation, the most important of which being the presence of coherent structures that have a dominant large length scale.

3. COMPUTATIONAL METHODOLOGY

For the computations, the solver Cobalt from Cobalt Solutions, LLC, was used [13]. It is a code which solves the compressible Navier–Stokes equations using a cell-centered finite volume approach applicable to arbitrary cell topologies (e.g. prisms and tetrahedra). It can achieve second-order accuracy in both time and space. In order to provide second-order accuracy in space,

DOI: 10.1002/fld

the spatial operator utilizes an exact Riemann solver [14] and, least-squares gradient calculations use QR factorization. It also employs TVD flux limiters to limit extremes at cell faces. A point implicit method using analytic first-order inviscid and viscous Jacobians is used for advancement of the discretized system. A Newton subiteration scheme is employed to achieve second-order accuracy in time.

At this Reynolds number, the attached boundary layer on the cylinder surface is laminar, but the wake is fully turbulent. The flow was simulated using large eddy Simulations with no explicit subgrid scale model. The numerical dissipation of the code was relied upon to remove the energy from the resolved scales, mimicking the effect of turbulence at the subgrid level, an approach also used by Hansen and Forsythe [15]. Although not all the small-scale turbulence can be simulated with this approach, it is adequate in terms of flow control applications. The flow at $Re=20\,000$ was simulated at a Mach number of $M=0.1$. The length to diameter ratio of the cylinder was $L/D=4$. Periodic boundary conditions were used on the computational surfaces at the cylinder ends, modified Riemann invariants were used as a farfield boundary condition, whereas a no slip, adiabatic wall was employed for the cylinder surface.

A time step of $\Delta t=0.576\times10^{-3}$ s corresponding to $\Delta t U/D=0.02$ non-dimensional time steps was employed. Time was non-dimensionalized by D/U. The total simulation time was 22 500 time steps, corresponding to 45 cycles of vortex shedding. With a shedding frequency of $f=3.47$ Hz, the Strouhal (St) number is 0.2 for this flow. The temporal resolution of the simulations was 500 time steps per von Karman shedding cycle.

In order to increase the stability, an advection damping coefficient of 0.01 was used in the computations. No damping was used for diffusion. To make the change of the variables at every time step converge, three Newton subiterations were used. As an initial perturbation to trigger the unsteadiness in the flow simulations, the incoming flow was skewed by an angle of attack of 1°.

The grid is an unstructured grid consisting of clustering of prismatic cells in the boundary layer and tetrahedral cells outside the boundary layer. It was generated by Gridtool/VGRID using the method of Morton *et al.* [16]. These type of grids were successful for detached eddy simulations of several applications including high Reynolds number separated flows [16]. The minimum cell height is $y/D=5\times10^{-4}$ and the y^{+}_{average} (average non-dimensional first cell height for the boundaries) is around 0.3. The grid has 879 603 cells. The farfield boundaries are 20 diameters away from the cylinder surface. The CFD model was validated using experiments performed at US Air Force Academy and experimental studies reported in citations. A grid refinement study and a time resolution study were also performed for the validation of the CFD model, using another grid with 2.5 million cells. The details of the computations and experiments were presented by Aradag [17] and Seidel *et al.* [18].

According to the results of the computations, time-averaged drag coefficient is equal to 1.20, which is within the range of the experimental results in literature [17]. The end of the length of the vortex formation region is defined as the peak in the turbulent intensity distribution. The computed value for the length of the vortex formation region is within 1% and the peak magnitude of turbulent intensity is within 3% of the average of the measured results in literature [17].

For the POD procedure, the data from five vortex shedding cycles each including 10 snapshots of data were used, which is adequate for this type of analysis according to a study by Barber and Ahmed [19].

4. MOTIVATION FOR NEW APPROACHES TO IDENTIFY LARGE-SCALE STRUCTURES

From a flow physics perspective, the circular cylinder wake at a Reynolds number of Re = 20 000 features laminar boundary layer flow over the front portion of the cylinder up to the separation point. The separated flow near the cylinder contains the fundamental von Karman vortices, which rapidly break down due to streamwise vortices that are superimposed on them. Further downstream, the Karman vortices break down into smaller and smaller turbulent structures. An instantaneous snapshot of isosurfaces of the spanwise component of vorticity is shown in Figure 1. The roll-up

DOI: 10.1002/fld

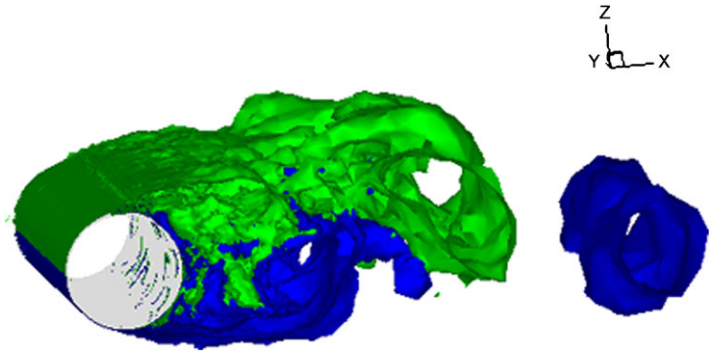

Figure 1. Iso-surfaces of spanwise vorticity, lightshade = 20 1/s, darkshade = −20 1/s.

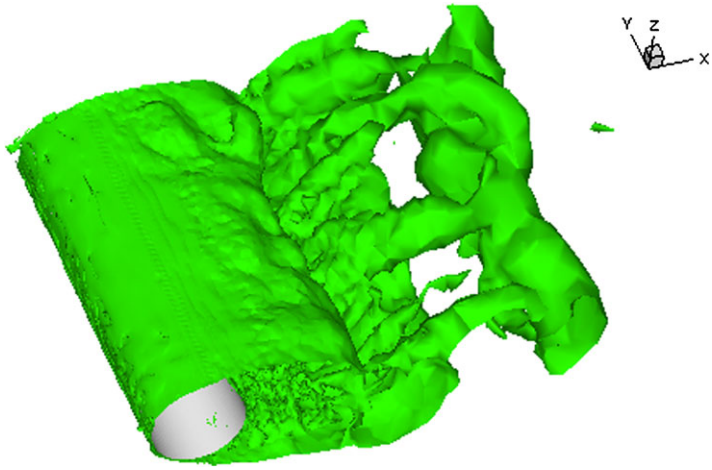

Figure 2. Total vorticity isosurfaces, 30 1/s.

of the boundary layer into the von Karman vortices can be seen, as well as the streamwise vortices that are present. The streamwise vortices can be seen more clearly in the instantaneous snapshot of total vorticity in Figure 2. The streamwise vortices that arise due to a secondary instability occurring beyond a Reynolds number of 260 [20], shown in Figure 2, modulate the vortex shedding with a spanwise wavelength of about one cylinder diameter.

Given a flow field like the one shown in Figures 1 and 2, the estimation problem for a typical control strategy targeting large structures, in particular the von Karman vortices, is to estimate the formation of the fast vortices described above correctly without being influenced by the smaller-scale turbulent motion in the flow. This estimation problem is aggravated by two additional issues. First, while the Karman vortex shedding problem is nominally two-dimensional, it also features a spanwise large wavelength shedding of vortices phases (Noack *et al.* [21]). Many different wavelengths are amplified, and there is no distinct difference in amplification rate. This spanwise phase variation makes it difficult to develop a correct POD-based spatial model of the flow, since POD will decompose these different spanwise distributions into different modes. From a controls perspective, this poses a problem, since a controller would have to address each of these similar, but distinct modes of comparable energy content separately. It would be preferable to characterize the flow with a two-dimensional POD mode plus a spanwise phase distribution instead. However, due to the von Karman vortex shedding by the streamwise vortices, a 2D approach is insufficient to characterize the wake flow simply by two-dimensional modes. Additionally, the characterization of the 2D shedding modes is hampered by the breakdown of these structures into smaller vortices. Figure 3 illustrates this problem. It shows spanwise vorticity contours for three different spanwise

DOI: 10.1002/fld

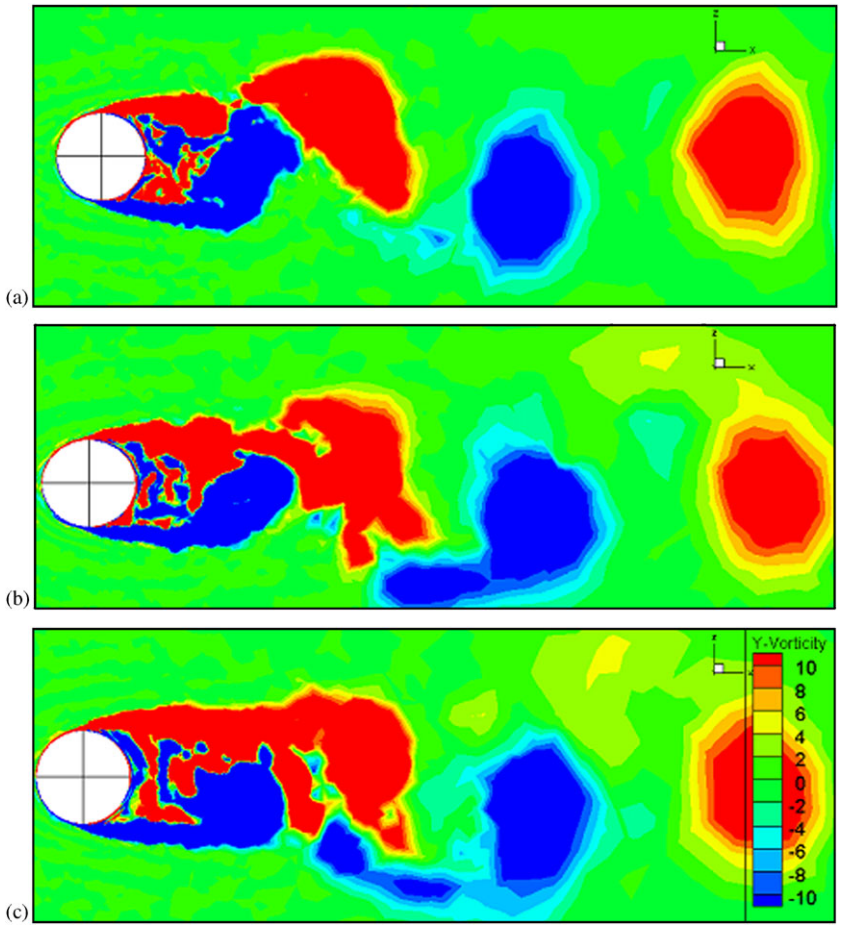

Figure 3. Spanwise vorticity contours on planes: (a) $y/D=1$; (b) $y/D=2$ (centerplane); and (c) $y/D=3$.

planes. Human eye can easily separate the large-scale structures such as the von Karman vortices from the rest of the flow and it can easily find the difference between the contours shown for several spanwise planes. However, a mathematical procedure like POD does not employ the spatial averaging performed instantaneously by the human brain. As a result, POD will not distinguish and identify structures by size, but rather group structures in a most energy optimal fashion. Unfortunately, this behavior is counterproductive for feedback flow control, where one would like to distinguish and control physically distinct structures, although POD is still necessary to obtain the mode amplitudes which are necessary for estimator and controller development.

Performing a POD of the entire 3D flow field reveals even more problems. Figure 4 shows the first four POD modes of streamwise velocity (U) from the 3D POD analysis of flow, performed using all the grid points in the CFD simulation, demonstrating the inability of POD to distinguish structures in a turbulent flow field like the one at hand. Since POD does not consider spatial size of any of the structures, none of the modes shown in Figure 4 reflects the von Karman vortex street only. Instead, each mode features a superposition of the von Karman vortex shedding, the streamwise vortices and the small-scale turbulence. This feature makes the POD modes shown in Figure 4 unsuitable for both identification and feedback control of these flow structures.

Since the small-scale turbulent motion is not the main item of interest in modeling of this flow field for the purpose of feedback control, a spatial filtering approach is an obvious choice to improve the POD results shown in Figure 4 with the goal of identifying the different flow features in separate modes. The goal would be to remove small-scale turbulent motion from the flow field, while retaining the large structures of interest to the flow control problem. To investigate the feasibility of

DOI: 10.1002/fld

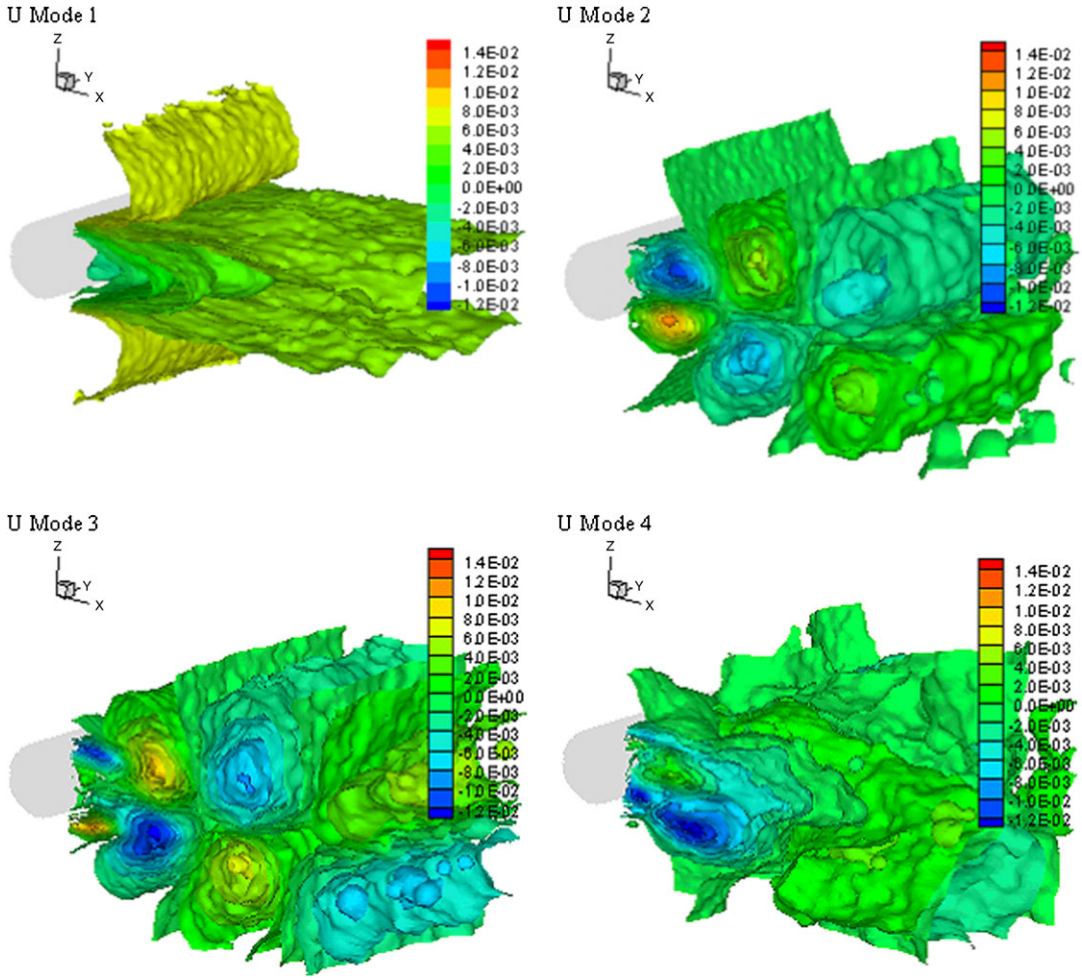

Figure 4. Isosurfaces of streamwise velocity modes 1–4.

this procedure, the flow field shown in Figures 1–3 was subjected to a spatial, linear interpolation procedure with an equidistant grid spacing of 0.05 cylinder diameters in the y-(spanwise), and z-directions, and 0.1 cylinder diameters in x (streamwise) direction. This interpolation serves two purposes. First, it organizes the unstructured grid-based simulation data into a structured data block of equidistant spacing. Second, it removes the small turbulent structures evident in Figures 3 and 4 through implicit spatial filtering with a stencil width equal to the grid size of the interpolation grid.

5. METHODOLOGY

The idea of harmonically filtering the data is natural. It has been used in a number of reduced order flow modeling approaches. For example, Iqbal and Thomas [22] used pre-filtering for noise removal from measurements and as an anti-aliasing tool. An interesting research performed by Prazenica *et al.* [23] demonstrated that POD analysis coupled with spatial filtering is an effective tool for analyzing scanning laser Doppler vibrometry data in fault detection applications. Scanning laser Doppler vibrometry experiments have been conducted in order to identify structural faults in frescoes at the US Capitol. In these experiments, the artwork is subjected to force excitations over a range of frequencies and a laser vibrometer is used to measure the velocity response of the structure over an array of spatial locations. At each frequency, a two-dimensional spatial image of

DOI: 10.1002/fld

the force–velocity transfer function is obtained. The use of POD, to identify coherent features in the structural response is described in their study. It is shown that the response can be characterized in terms of only a few POD modes corrupted by spatially varying noise. Therefore, the use of spatial filtering techniques is also explored for removing this noise from the measured force–velocity transfer functions prior to performing the POD analysis. Several wavelet bases are used to filter the images. In addition, wavenumber filters, which essentially act as low-pass filters, are also employed [23]. Galerkin models with mixed Fourier and POD expansions have been widely used to filter stochastic effects by imposing symmetry. Examples include Aubry *et al.* [24], Smith *et al.* [25], Johansson *et al.* [26] and Gamard *et al.* [27].

Dowell and Hall [28] used reduced order modelling for fluid–structure interaction. They used temporal pre-filtering to impose periodicity and indirectly remove small and stochastic spatial structures. Attar *et al.* [29], Gamard *et al.* [27] and Tadmor *et al.* [30] are examples for temporal pre-filtering that helps removing small structures.

Alternative filtering methods have also been utilized by several researchers. For example, wavelet filters used by Farge *et al.* [31] is a good example. Their study compares the filtering used in Coherent Vortex Simulation decomposition with an orthogonal wavelet basis with POD or Fourier filtering.

In this study, two different methods were applied to the spatially filtered data obtained from the simulations in order to identify the von Karman vortices. Since the Karman vortex shedding mode is a two-dimensional flow feature, one may postulate that it can be modeled using a two-dimensional mode that is allowed to vary in phase and intensity across the span. The Hybrid Filtered POD approach [32] is the first approach used in this study. Data from five shedding cycles of the simulation were used to develop the two-dimensional spatial modes. The data were organized in y (number of spanwise planes) times t (time) snapshots where each spanwise plane was treated as one snapshot for a POD procedure. In several investigations the POD snapshots are centered around the mean flow; in several others, including this study, they are not. POD can be performed in two different ways: the mean can be subtracted and the modes can be found after this or no mean flow is subtracted from the original flow data. When the mean flow is not subtracted, the first mode shows the mean flow as in the present study. Although the two procedures seem different, they are similar procedures after the mean is subtracted.

3D Filtered POD [33, 34] is a method where 3D POD procedures are applied to the spatially filtered data from the simulations. Iso-surfaces of velocity of 3D POD modes 2–3 obtained from Re=20 000 simulations after the application of 3D POD to the spatially filtered data are shown in Figure 5. Von Karman vortices can be identified in the second and third modes of Figure 5. This

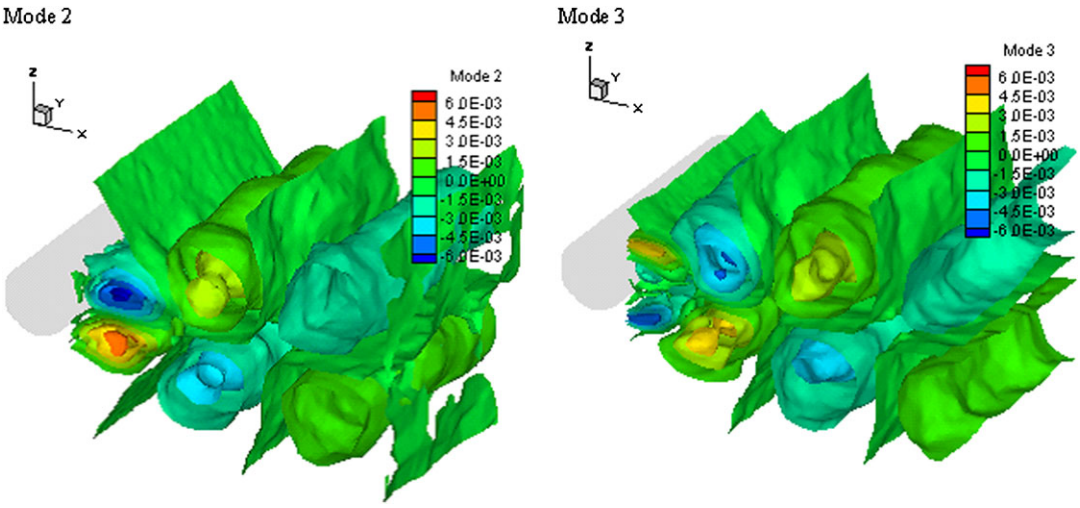

Figure 5. Iso-surfaces of streamwise velocity (U) of 3D Filtered POD modes 2–3 (m/s).

DOI: 10.1002/fld

shows that a spatial, linear interpolation procedure is able to remove some of the 3D structures present in the flow, allowing 2D structures to be identified in the flow.

Using 3D POD on properly spatially filtered data is a promising way of identifying the two-dimensional large-scale structures in the flow. However, in order to use this procedure, special care must be given to cutoff wavelength of the filter. The data can further be down-sampled using equidistant grid spacing. However, when the data are down-sampled, it is not possible to know how much structured filtering is necessary and what the filtering grid size in each direction needs to be without trial and error. Furthermore, we cannot be sure not to lose any significant information necessary for flow control when we filter the data further with increasing equidistant grid spacing. Therefore, a systematic procedure is necessary to spatially filter the data and analyze the results. A spatial filtering method based on FFT was developed and applied to the data obtained from the simulations.

FFT is an efficient algorithm to compute the discrete Fourier transform and its inverse. FFT is of great importance to a wide variety of applications, especially for digital signal processing. It is usually performed on time histories of data to change the signal value from time domain to frequency domain. In this study, FFT analysis of the data is performed in spatial directions to change the signals in spatial domain to wave number domain. The filtering procedure is as follows:

1. The flow field is subjected to a spatial, linear interpolation procedure with an equidistant grid spacing of 0.05 cylinder diameters in the y (spanwise), and z directions, and 0.1 cylinder diameters in the x (streamwise) direction.
2. The data are organized in $(yXzXt)$ different lines, extending in the streamwise (x) direction.
3. FFT of each line is performed to transform the data from a spatial domain to a wave number domain.
4. The spectrum obtained from the FFT analysis is examined and the large wave number (small wavelength) part of the data is omitted, considering the fact that the large-scale structures necessary for flow control have large wavelength, producing more energy in the power spectrum obtained from the FFT analysis. Only the first dominant wave number in the spectrum was kept for further analysis of the data.
5. An inverse FFT is applied to the new data set to reconstruct the flow field using only the low wave number part of the data.
6. The data, filtered in the streamwise (x) direction using the procedure 2–5, are organized as several lines in spanwise (y) direction and the procedure 2–5 is applied on the new data set.
7. Same procedure 2–5 is applied to the data in the remaining direction (z).

After the data are filtered according to wavelengths using this three-dimensional FFT procedure (1–7), POD is applied to the filtered three-dimensional data and the results are investigated in terms of modes, mode energies and amplitudes. This procedure named as 3D FFT-based Filtered POD is the second method used in this study.

6. RESULTS

Figure 6 shows the spatial modes obtained from the data using Hybrid Filtered POD approach. Since the mean flow was not subtracted, the first mode represents the mean flow, while modes 2 and 3 represent the von Karman vortex street. All these modes bear a striking resemblance to the modes that were derived from either PIV measurements or 2D CFD simulations reported by Siegel *et al.* [34], showing the capability of Hybrid Filtered POD in separating the large-scale two-dimensional structures from 3D small-scale turbulence.

The energy content of the 3D POD applied to the data at all the CFD grid points without any filtering and the POD modes obtained using the Hybrid Filtered POD method are compared in Figure 7. The two von Karman modes are of similar energy content, and capture more energy than their 3D counter parts, which shows that the Hybrid Filtered POD approach does a better job than

DOI: 10.1002/fld

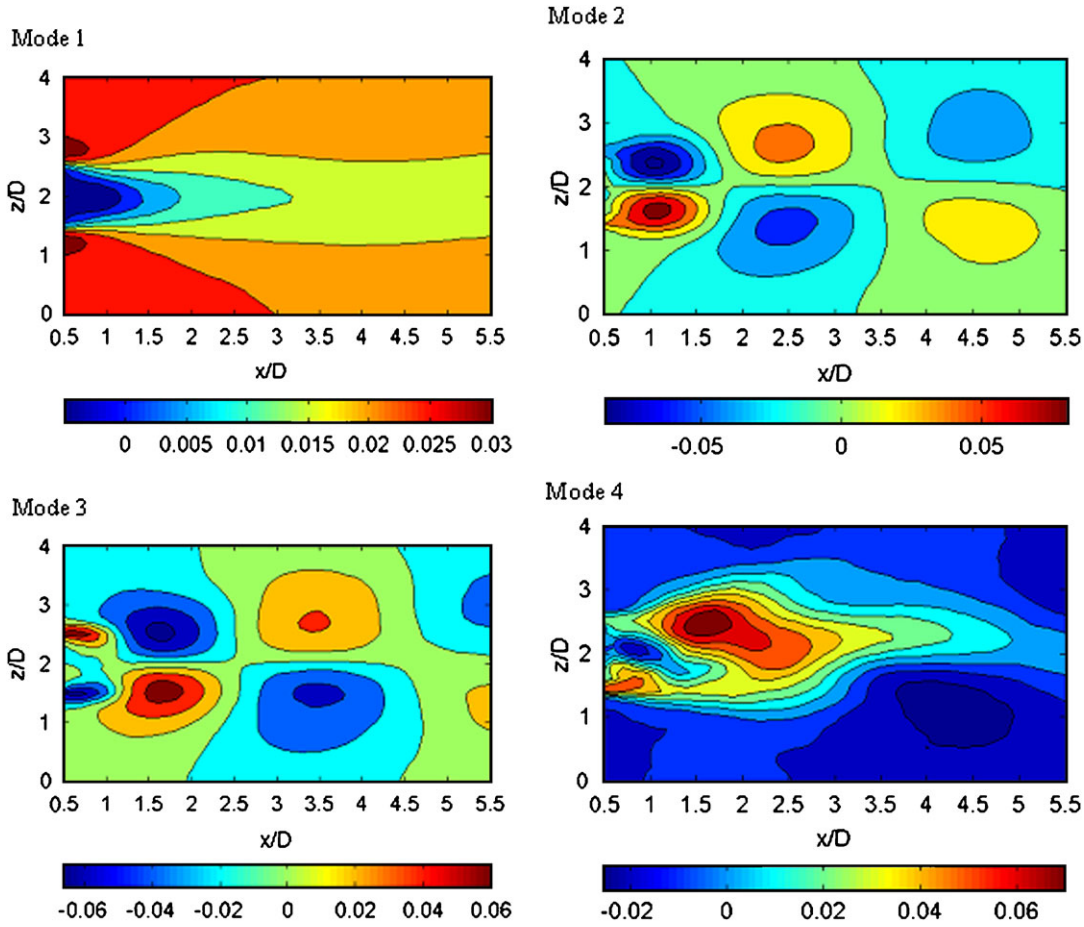

Figure 6. Hybrid Filtered POD modes, Iso-contours of streamwise velocity (m/s).

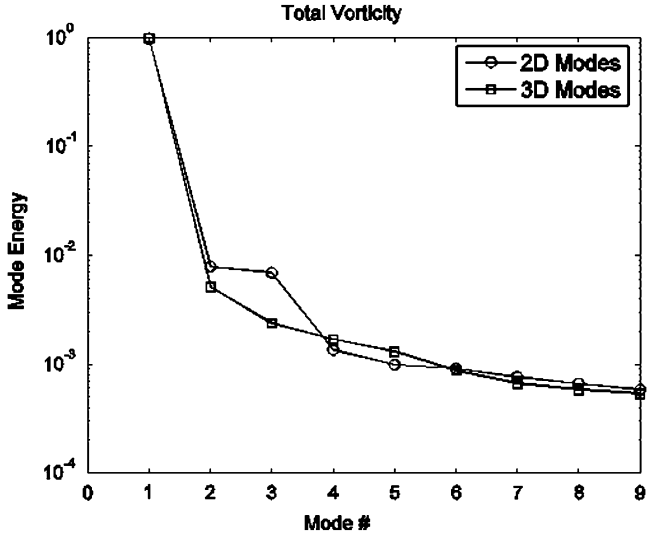

Figure 7. Energy content comparison of Hybrid Filtered POD and 3D POD modes.

DOI: 10.1002/fld

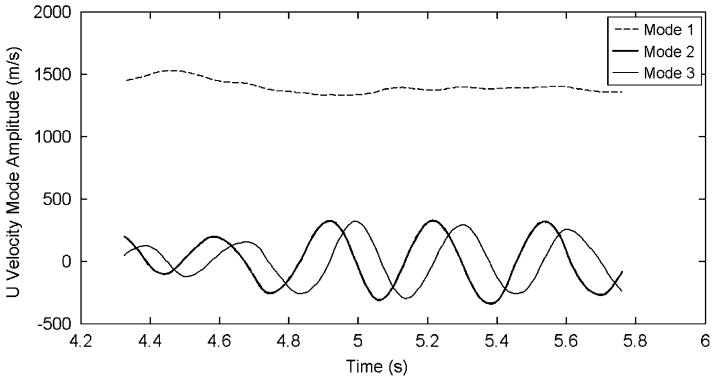

Figure 8. 2D time coefficients on centerline of model, $Re = 20000$.

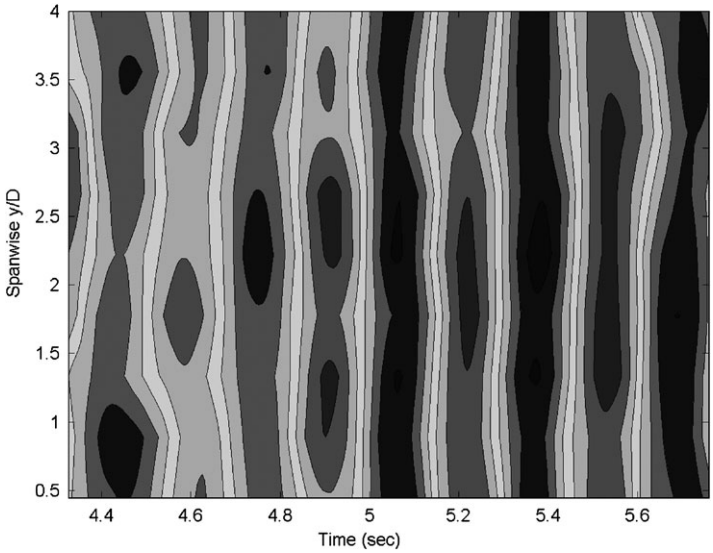

Figure 9. 2D time coefficient of POD mode 2 (1st Karman mode) as contour plot across model span.

POD directly applied to three-dimensional flow to separate the von Karman vortex street from the rest of the flow.

Inspection of the temporal coefficients of the 2D POD at the centerline of the model shown in Figure 8 shows the mean flow mode (Mode 1) to be non-fluctuating with approximately constant amplitude. The two von Karman modes are approximately sinusoidal with slightly varying amplitude and frequency. These variations are most likely due to the spanwise traveling nature of the phase distribution of the vortex shedding as can be seen in Figure 9. While the shedding is almost parallel to the cylinder, it features a spanwise amplitude variation and slight phase variations, especially later in the simulation. Most remarkable, however, is the ability of the Hybrid Filtered POD model to identify in a quantitative fashion the large-scale structures associated with the Karman vortex street and their spanwise amplitude and phase variations. This capability of the hybrid modeling approach is of great importance for the development of flow estimation and control tools.

FFT filtering was performed using the procedure explained in the previous section. Several cut-off wave numbers were tested in order to decide which wave lengths would be included in the reconstruction of the data using inverse FFT. The von Karman vortices are large-scale structures with large wave length compared to the small-scale turbulence in the flow. Therefore, the first peak corresponding to the highest peak obtained from the FFT analysis of the data would constitute

DOI: 10.1002/fld

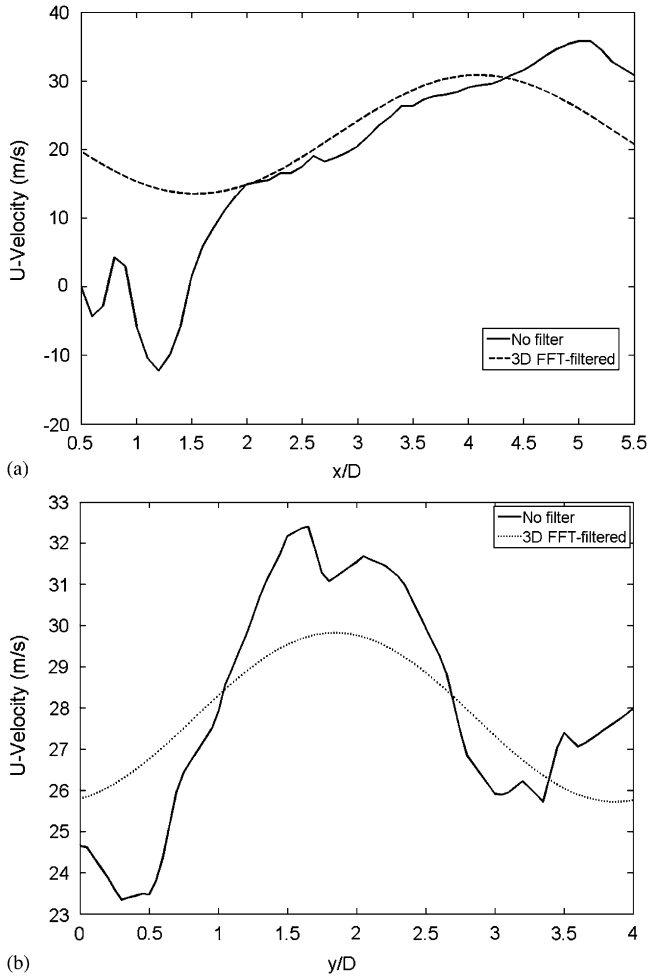

Figure 10. Instantaneous streamwise velocity (U) before and after filtering (a) U versus x/D at $y/D=4$ and $z/D=0$ and (b) U versus y/D at $x/D=4.5$, $z/D=0$.

the von Karman vortex street since it has the lowest wave number and largest wave length in the flow. Only the first (highest) peak in the FFT in all three directions was kept in the data after the filtering procedure.

Figure 10 shows the unfiltered and filtered U-velocity plots after the application of FFT-based filtering. The small-scale fluctuations in the velocity for the unfiltered case are not present in the FFT-based filtered case. Figure 11 shows a typical power spectrum obtained from the FFT analysis of a U-velocity signal such as the one shown in Figure 10(a), labeled as no filter. Such a power spectrum is cut after the highest (first) peak and inverse FFT is applied to it to obtain a filtered velocity signal shown in Figure 10(a), labeled as 3D FFT filtered.

The 3D Filtered POD procedures were applied to the data for two different cases, one of them being filtering the data in streamwise (x) direction only and the second one being filtering the data in all three directions. Figure 12 shows the energy content of the U-velocity modes for the unfiltered and 1D (x) and 3D (x, y, z respectively) FFT-filtered cases. As seen in Figure 12, the energies of the filtered cases in higher order modes are lower than the original case, allowing the dominant features of the flow to be represented with less number of modes. For the filtered cases, the energy contents of modes 2 and 3 represent a Karman vortex street with equal energies, whereas it is evident from the energy content distribution that the Karman modes are mixed with other structures for the unfiltered case, where the energies of modes 2 and 3 are not equal to each other.

DOI: 10.1002/fld

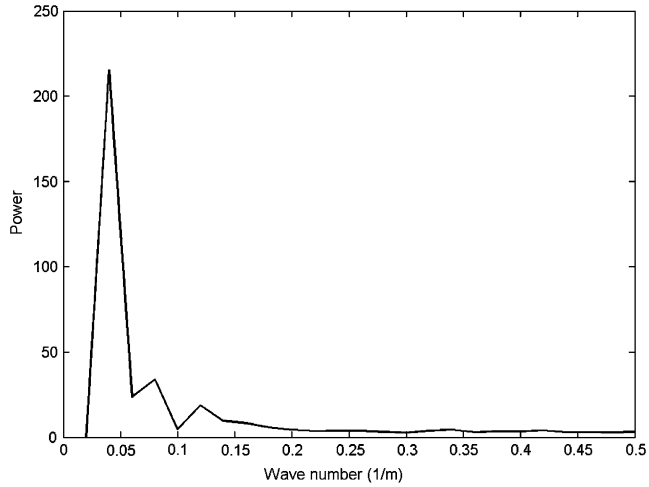

Figure 11. Typical power spectrum obtained from the FFT analysis of streamwise (U) velocity (at $y/D=4$ and $z/D=0$).

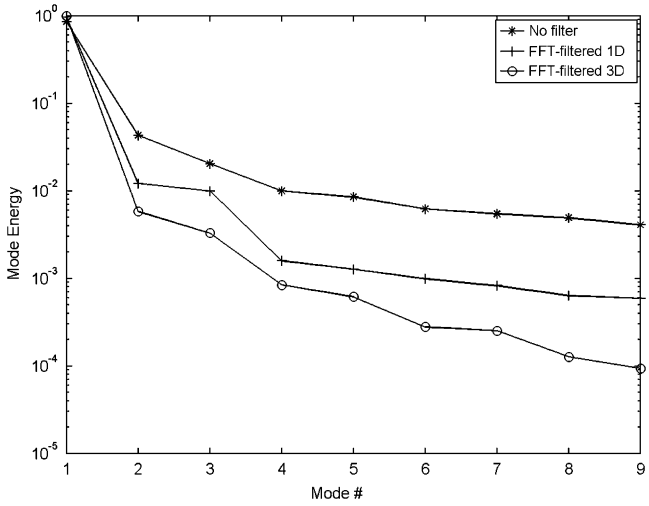

Figure 12. Energy content comparison of filtered and not filtered streamwise velocity (U) modes 1–9.

Figure 13 shows streamwise velocity mode 4 for two different filtering cases. The data were filtered with an equidistant grid spacing of 0.05 cylinder diameters in the y (spanwise), and z directions, and 0.1 cylinder diameters in the x (streamwise) direction without FFT for the first case. For the second case, the filtered data set was also processed through an FFT filtering procedure in streamwise direction. Although the small-scale structures are eliminated in the streamwise direction using an FFT procedure, it is evident from Figure 13 that several spanwise small-scale structures still exist in the data set after filtering in one direction. For this reason, the data were further processed through the FFT procedure in all three directions.

Figure 14 shows the second and third streamwise velocity modes (Karman modes) obtained from FFT-based filtering in all directions where the data set is completely filtered from the small-scale fluctuations, showing the von Karman vortex street only, as opposed to modes in Figure 4 obtained without any filtering.

The mode amplitudes for modes 1, 2 and 3 are shown for the unfiltered and 3D FFT-filtered cases in Figure 15. The amplitudes obtained from the FFT-based 3D Filtered POD shows the time signals of the von Karman vortices that are 90° apart free of small-scale turbulent structures

DOI: 10.1002/fld

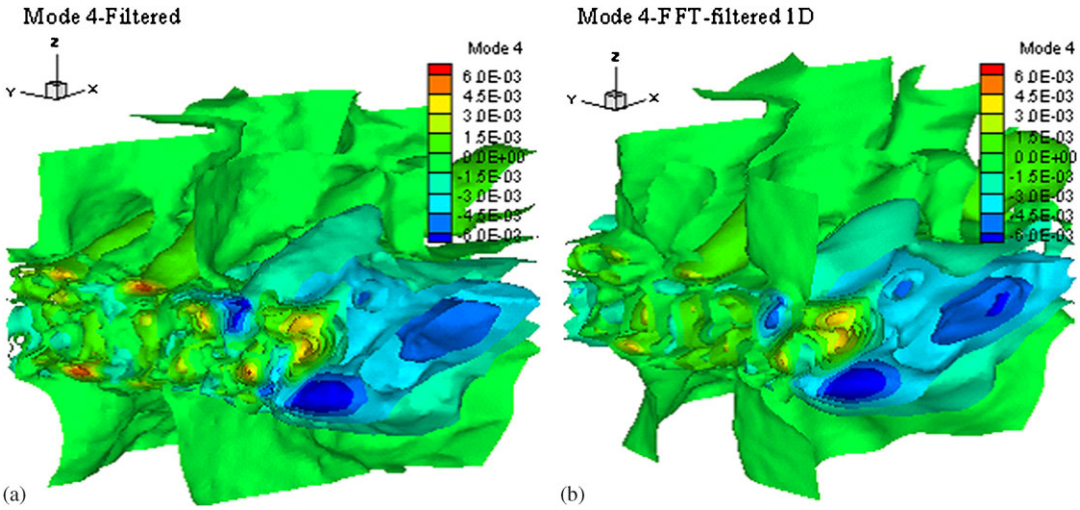

Figure 13. Isosurfaces of streamwise velocity (U) modes 4 for the data sets: (a) Filtered with an equidistant grid spacing in every direction and (b) FFT-filtered in x direction.

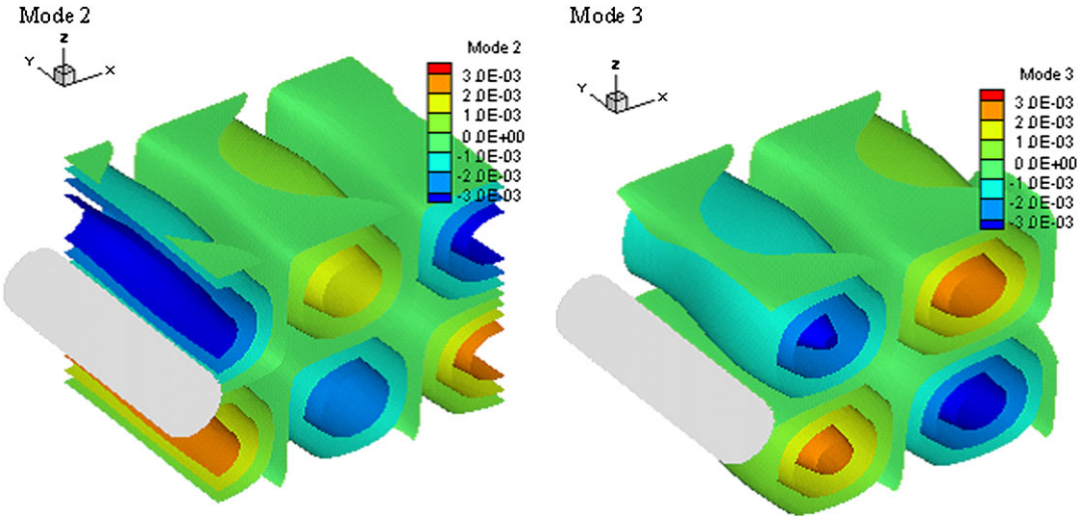

Figure 14. Isosurfaces of 3D FFT-filtered streamwise (U) velocity modes 2–3 (Karman modes).

present in the flow. The magnitudes and phase of the Karman vortices are not as clear for the case where no filtering is applied.

7. CONCLUSIONS AND RECOMMENDATIONS

Two different methods were applied to the spatially filtered data obtained from the simulations of turbulent flow over a circular cylinder at a Reynolds number of 20 000 in order to identify and sort the two-dimensional structures (i.e. von Karman vortex street) present in the flow.

The first method is Hybrid Filtered POD approach similar to the one pioneered by Ma and Karniadakis [12]. The ability of this method to identify in a quantitative fashion the large-scale structures associated with the von Karman vortex street and their spanwise amplitude and phase variations is remarkable. This capability of the hybrid modeling approach is of great importance for the development of flow estimation and control tools.

DOI: 10.1002/fld

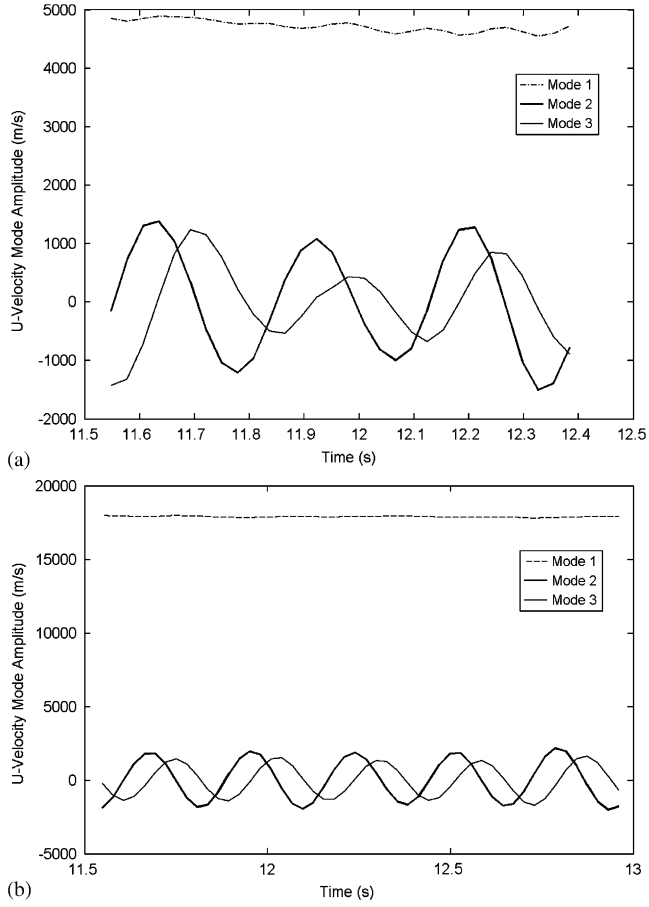

Figure 15. U mode amplitudes for (a) Not filtered and (b) 3D FFT-filtered cases.

The next method used is called 'FFT-based 3D Filtered POD' where 3D POD procedures were applied to the spatially filtered data from the simulations. This approach is also promising for identifying the two-dimensional structures such as the Karman vortex street, provided that a proper filter is used. The idea is to eliminate the structures that are below a certain size. First the sizes of the structures in the flow need to be identified qualitatively to decide on what size of filtering to use initially. A spatial filtering method based on FFT is developed and applied to the data to identify the large-scale structures better from the POD analysis of the three-dimensional data. 3D FFT-based Filtered POD approach is able to capture the large-scale features of the flow, such as the von Karman vortex street, while not being contaminated by small-scale turbulent structures, which makes it an alternative means for modeling of 3D flows. The filtering procedure needs to be repeated until most of the small-scale structures are eliminated qualitatively. Using FFT-based spatially filtered data for POD is a promising way of obtaining the modes and mode amplitudes necessary for flow state estimation and control of complex turbulent three-dimensional flow fields, since the large-scale structures that also cause the small-scale structures in the flow to develop can be separated from the rest of the flow and the time signals obtained from them can be used for estimation and controller development.

Hybrid Filtered POD provides spanwise phase. However, the FFT filtered POD approach works for 3D geometries, which makes it a promising alternative to the Hybrid POD method for the modeling of 3D flows.

The next step in this research is to perform flow state estimation using Artificial Neural Networks and to design a controller based on the information obtained using the two methods developed in this study.

DOI: 10.1002/fld

NOMENCLATURE

D	diameter of the cylinder
L	spanwise length of the cylinder
M	Mach number
Re	Reynolds number
S	strain rate tensor
St	Strouhal number for the vortex shedding
U	free stream velocity
f	shedding frequency of the flow
y^+_{average}	average non-dimensional first cell height
Δt	time step

ACKNOWLEDGEMENTS

This research was supported by Air Force Office of Scientific Research under grant FA-955005C0048. The CFD computations were performed at USAFA Blackbird computer cluster. The authors thank the Modeling and Simulation Research Center directed by Dr Keith Bergeron and Dr Jim Forsythe from Cobalt Solutions for the computational support.

REFERENCES

1. Cohen K, Siegel S, McLaughlin T, Gillies E, Myatt J. Closed-loop approaches to control of a wake flow modeled by the Ginzburg–Landau equation. *Computers and Fluids* 2005; **34**:927–949.
2. Gillies EA. Low-dimensional control of the circular cylinder wake. *Journal of Fluid Mechanics* 1998; **371**: 157–178.
3. Park DS, Ladd DM, Hendricks EW. Feedback control of a global mode in spatially developing flows. *Physics Letters A* 1993; **182**:244–248.
4. Cohen K, Siegel S, McLaughlin T. Control issues in reduced-order feedback flow control, invited lecture at session titled 'Closed-Loop Flow Control: Algorithms and Applications'. *42nd AIAA Aerospace Sciences Meeting*, Reno, Nevada, January 2004. AIAA Paper 2004-0575.
5. Noack BR, Tadmor G, Morzynski M. Actuation models and dissipative control in empirical Galerkin models of fluid flows. *2004 American Control Conference*, *Paper FrP15.6*, July 2004.
6. Noack BR, Tadmor G, Morzynski M. Low-dimensional models for feedback flow control. Part I: empirical Galerkin models, *2nd AIAA Flow Control Conference*, Portland, Oregon, AIAA-2004-2408, June 2004.
7. Tadmor G, Noack BR, Morzynski M, Siegel S. Low-dimensional models for feedback flow control. Part II: observer and controller design, *2nd AIAA Flow Control Conference*, Portland, Oregon, AIAA Paper 2004-2409, June 2004.
8. Roussopoulos K. Feedback control of vortex shedding at low Reynolds numbers. *Journal of Fluid Mechanics* 1993; **248**:267–296.
9. Ma X, Karniadakis G. A low-dimensional model for simulating three-dimensional cylinder flow. *Journal of Fluid Mechanics* 2002; **458**:181–190.
10. Unal M, Rockwell D. On vortex shedding from a cylinder, part 1: the initial instability. *Journal of Fluid Mechanics* 1988; **190**:491–512.
11. Karniadakis GE, Triantafyllou. Three dimensional dynamics and transition to turbulence in the wake of bluff objects. *Journal of Fluid Mechanics* 1992; **238**:1–30.
12. Williamson C. Three dimensional wake transition. *Journal of Fluid Mechanics* 1996; **328**:345–407.
13. Strang WZ, Tomaro RF, Grismer MJ. The defining methods of Cobalt60: a parallel, implicit, unstructured Euler/Navier–Stokes flow solver. *37th Aerospace Sciences Meeting and Exhibit*, Reno, NV, AIAA 99-0786, January 1999.
14. Gottlieb JJ, Groth CPT. Assessment of Riemann solvers for unsteady one-dimensional inviscid flows of perfect gases. *Journal of Computational Physics* 1988; **78**:437–458.
15. Hansen R, Forsythe J. Large and detached eddy simulations of a circular cylinder using unstructured grids. *41st Aerospace Sciences Meeting and Exhibit*, Reno, Nevada, AIAA-2003-775, January 2003.
16. Morton SA, Forsythe JR, Squires KD, Wurtzler KE. Assessment of unstructured grids for detached eddy simulation of high Reynolds number separated flows. *Proceedings of the Eight International Conference on Numerical Grid Generation in Computational Field Simulations*, Honolulu, HI, June 2002.
17. Aradag S. Unsteady vortex structure behind a three dimensional turbulent cylinder wake. *Journal of Thermal Science and Technology* 2009; **29**(1):91–98.
18. Seidel J, Cohen K, Aradag S, Siegel J, McLaughlin T. Reduced order modeling of a turbulent three-dimensional wake. *37th AIAA Fluid Dynamics Conference and Exhibit*, Miami, FL, June 2007. AIAA 2007-4503.

DOI: 10.1002/fld

19. Barber T, Ahmed H, Abdel Shafi NY. POD snapshot data reduction for periodic fluid flows. *43rd AIAA Aerospace Sciences Meeting and Exhibit*, Reno, NV, January 2005. AIAA 2005-287.
20. Williamson CHK. Vortex dynamics in the cylinder wake. *Annual Review of Fluid Mechanics* 1996; **28**:477–539.
21. Noack B, Eckelmann H. A global stability analysis of the steady and periodic cylinder wake. *Journal of Fluid Mechanics* 1994; **270**:297–330.
22. Iqbal MO, Thomas FO. Coherent structure in a turbulent jet via a vector implementation of the proper orthogonal decomposition. *Journal of Fluid Mechanics* 2006; **571**:281–326.
23. Prazenica R, Kurdila AJ, Vignola JF. Spatial filtering and proper orthogonal decomposition of scanning laser Doppler vibrometry data for the nondestructive evaluation of frescoes. *Journal of Sound and Vibration* 2007; **304**(3–5):735–751.
24. Aubry, Holmes P, Lumley JL, Stone E. The dynamics of coherent structures in the wall region of a turbulent boundary layer. *Journal of Fluid Mechanics* 1988; **192**:115–173.
25. Smith TR, Moehlis J, Holmes P. Low-dimensional models for turbulent planeCouette flow in a minimal flow unit. *Journal of Fluid Mechanics* 2005; **538**:71–110.
26. Johansson PB, George W, Woodward SH. Proper orthogonal decomposition of an axisymmetric turbulent wake behind a disk. *Physics of Fluids* 2002; **14**:2508. DOI: 10.1063/1.1476301.
27. Gamard S, George W. Application of a 'slice' proper orthogonal decomposition to the far field of an axisymmetric turbulent jet. *Physics of Fluids* 2002; **14**:2515. DOI: 10.1063/1.1471875.
28. Dowell EH, Hall KC. Modeling of fluid–structure interaction. *Annual Review of Fluid Mechanics* 2001; **33**: 445–490. DOI: 10.1146/annurev.fluid.33.1.445.
29. Attar PJ, Dowell EH, White JR, Thomas JP. Reduced order nonlinear system identification methodology. *AIAA Journal* 2006; **44**(8):1895–1904.
30. Tadmor G, Bissex D, Noack BR, Morzynsky M, Colonius T, Taira K. Temporal-harmonic specific POD mode extraction. *4th Flow Control Conference*, Seattle, WA, June 2008. AIAA paper 2008-4190.
31. Farge M, Schneider K, Pelegrino G, Wray AA, Bogallo RS. CVS decomposition of 3D homogenous turbulence using orthogonal wavelets. *CTR Summer Program 2000*, NASA/Stanford University, Stanford, CA, 2000; 305–317.
32. Siegel S, Aradag S, Seidel J, Cohen K, McLaughlin T. Low dimensional POD based estimation of a 3D turbulent separated flow. *45th AIAA Aerospace Sciences Meeting and Exhibit*, Reno, NV, January 2007. AIAA Paper 2007-0112.
33. Aradag S, Siegel S, Seidel J, Cohen k, McLaughlin T. Filtered POD based estimation of 3D turbulent separated flows. *46th AIAA Aerospace Sciences Meeting and Exhibit*, Reno, NY, January 2008. AIAA paper 2008-0554.
34. Siegel S, Cohen K, McLaughlin T. Feedback control of a circular cylinder wake in experiment and simulation (invited), *33rd AIAA Fluid Dynamics Conference*, Orlando, June 2003. AIAA 2003-3569.

DOI: 10.1002/fld